Impact of a reversible substation on energy recovery experienced on-board a train

Impact of a reversible substation on energy recovery experienced on-board a train

F. Cascetta[1], G. Cipolletta[1], A. Delle Femine[1],
J.Quintana Fernández[2], D. Gallo[1], D. Giordano[3], D. Signorino[3,4]

[1] *Università degli studi della Campania "Luigi Vanvitelli", Aversa (CE) – Italy, (antonio.dellefemine, daniele.gallo)@unicampania.it*
[2] *Metro de Madrid, C/ Néctar, 44 – 28022 (Madrid) jorge.quintana@metromadrid.es*
[3] *INRIM, strada delle Cacce 91- 10135, Torino – Italy, (d.giordano, d.signorino)@inrim.it*
[4] *Politecnico di Torino, c.so Duca degli Abruzzi Torino – Italy*

***Abstract* – European energy policy encourages the railway stakeholders to adopt technological solutions to reduce the railway transport emissions by 50% within 2030. To this aim, the dynamic braking combined with the adoption of reversible substations is one of the most promising solutions. To deepen the knowledge of this new technology in its practical application, this paper presents the results of a measurement campaign that has been conducted on-board of a train operating on the metro line that serves the city of Madrid, where a reversible substation was installed. The installed measurement system allows the accurate measurements of the energy flows and the losses. The monitoring has been performed both when the substation acts as reversible and when operates in a traditional way. The comparison could be used to quantify the impact of these technologies in a real application, providing information on energy saving in the different operating conditions and presenting a methodology to quantify them.**

Keywords – Electric Power and Energy Measurement, Railway system, Reversible Substation, energy saving, regenerative brake, dynamic braking.

I. INTRODUCTION

In the last years, European policy effort in shifting towards low-emission mobility are becoming more and more effective. The ambitious aim is to have greenhouse emission from transport, by mid-century, at least 60% lower than 1990 [1], [2]. Obviously, the European road map, to hit the target, requires the electrification of transports, the optimization of the whole transport system and the efficiency improvement. The White paper [1] fixes the objectives to be reached in 2050. Phase out in cities the use of 'conventionally-fuelled' cars; 50% of road freight over 300 km should shift to other modes such as rail or waterborne transport (target referred to year 1990); completion of a European high-speed rail network and, in the end, the majority of medium-distance passenger transport should go by rail. Therefore, the UE policy works towards a wider diffusion of electric railway/metro system, the nature of which is more environmentally friendly and energy-efficient than other modes, yet still capable of being even more so. The total amount of energy required for the European railway system is a huge number (78.9 TWh for EEA33 excluding Switzerland and Liechtenstein in 2018, [3]) but, because of the electric transport transition, such figure will dramatically increase. To achieve the ambitious objectives of reducing the CO2 emissions and, at the same time, to meet the growing demand for traffic, the energy efficiency of the railway system must be significantly enhanced [1].

One of the reasons that makes the electric railway system energy-efficient is the exploitation of the dynamic braking, that is the capability of an electric motor to recover energy during the braking phase [4]. This recovered energy can be consumed on board (by auxiliary systems for example) or reinjected on the overhead line. In DC railway systems, the common supply substations allow only a unidirectional energy flow (from the electrical grid to the trains) so the regenerated energy, once injected on the catenary, can be only reused by other adjacent trains that need energy at the same time. If this condition does not occur, the energy should be dissipated on board by dedicated rheostats to avoid excessive increasing of catenary voltage level [5]-[7]. Therefore, there is only a certain probability of energy recovery, and generally, a considerable part of this energy is dissipated. The amount of recovered energy depends by several factors, i.e. the braking effort, the number of braking events, the number of trains operating on the line, the supply configuration, etc. One of the solutions to increase the energy saving from braking is the adoption of energy storage devices installed near the railway line or on board. Since the braking energy presents high power peaks for short time, the strategy could be the use of supercapacitor banks. Given the available energy density they require a lot of space for their installation and dedicated power

[1] The results here presented are developed in the framework of the 16ENG04 MyRailS Project founded from the EMPIR program co-financed by the Participating States and from the European Union's Horizon 2020 research and innovation program.

electronic converters to adapt the system voltage to the storage voltage and to manage the reutilization of energy within a short time, in order to avoid self-discharge and maintain high efficiency, [11]. Another solution to exploit most of the energy produced by braking is the organization of the timetable. In literature there are numerous models that aim to coordinate the coasting, stop and start phases of the trains on the same line in order to synchronize the braking with the traction phases [12]-[22]. An interesting technical solution is provided by the Reversible Substation (RSS) [23]. Thanks to this supply solution, the energy generated by dynamic braking and not absorbed by other trains, is injected to the upstream AC power distribution network, making the substation a prosumer. At present, this technology is much more diffused in metro and tram systems than the railway ones, since the lower power of the substations which makes easier the design and the implementation of a RSS. Numerical simulations provide interesting information on the amount of energy that is actually wasted in rail systems, up to 40 % of the traction energy can be wasted [12], while a measurement campaign carried out on-board an Italian locomotive for railway commuter service provides a wasted energy up to 20 % [24].

Nowadays, even more RSSs are installed in metro and railway systems. Nevertheless, the scientific literature provides many results based on simulation to estimate energy saving due to the RSSs and very few valid and reliable data aimed at quantifying the actual energy that can be saved adopting this technology in a real application. An impact Percentages ranging between 15 % and 20 % for the computed energy efficiency impact of RSS are quite common. Interesting data collected on-site are provided by the review work published by Douglas & al. [12]. The single RSS installed in the Bilbao metro shown energy savings which surpassed predicted results. In this case, the single prototype installed on high traffic section reduced annual substation consumptions by 11.3 % when originally savings of only 8.3 % were theorized [12]-[25].

In order to contribute to the enhancement of scientific knowledge, this research proposes and applies a method for the analysis of the energy efficiency impact of the RSS from train operator and train designer point of view. In details, the paper presents the results of the statistical analysis of the energy flows exchanged between train and overhead contact line performed on data gathered from a measurement campaign carried out on a metro-train in commercial service for the analysis of in presence of a RSS. To this end, a specific measurement system, able to perform a complete energy analysis, was developed and installed on board a train operating on a metro line that serves the city of Madrid, where a RSS was installed, [26]. This activity is part of the metrology research project EMPIR 16ENG04 MyRailS, [27]. In the following, in Section II the line and train subject of the research will be illustrated. Section III describes measurement system together with the measurement points. Experimental results with numerical analysis and some authors' considerations on the measurement carried out is reported in Section IV.

II. SUBWAY LINE AND TRAIN UNDER ANALYSIS

To reduce management costs and the ecological footprint of the metro of Madrid, one of the substations was modified adding a DC/AC converter of 2 MVA in anti-parallel to a traditional, already present rectifier of 3 MVA. In this way, a bidirectional flow of energy was obtained with minimal modifications of the existing electric system, see Fig. 1.

The line under analysis goes from Hospital Infanta Sofia to Tres Olivos with 11 stations (see Fig. 2) and covers a distance of about 15 km with a roundtrip journey that lasts about 47 minutes. The catenary is supplied by five substations, that are placed in: Hospital Infanta Sofia, Baunatal, La Moraleja, Las Tablas and Tres Olivos. The DC/AC converter has been installed at the substation of La Moraleja located in the middle of the line. It is also worthwhile noting that, at the time of measurement campaign, the RSS was not operating at full capacity because the energy provider has not yet allowed to feed energy at the delivery point into the main power grid. Therefore, the system can recover only the energy that can be used on the Metro de Madrid AC network and this can, obviously, limit the amount of the recoverable energy. Nevertheless, it is interesting to evaluate the impact of the reversible station under these conditions, although the recovery effectiveness is expected to improve when this limitation will be removed.

The energy monitoring has been carried out on-board a train in commercial service on that line. It is a subway train with three cars, model "S9000 3 CARS SS3", whose main mechanical characteristics are reported in [26]. From the electrical point of view, its nominal line voltage is 1500 V DC and the maximum current absorption is of 1650 A. The train under test has two traction units supplied by two independent pantographs. The two traction units are controlled with identical commands and they work in nearly the same conditions, so it is possible to assume that energy flows are nearly identical. Therefore, it was decided to install the monitoring system on a single unit so, in the following, all the discussion and results will be referred to a single traction unit. In order to obtain an evaluation of power and energy absorbed by the whole train, it is possible to simply scale by two the values obtained by the single traction unit.

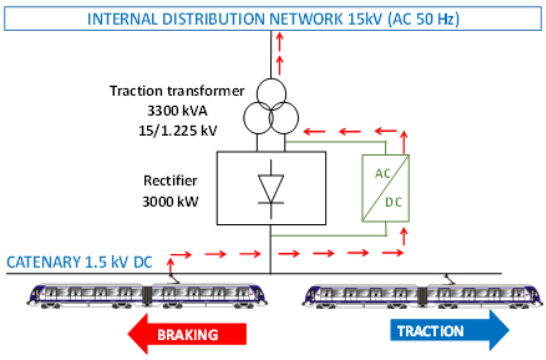

Fig. 1. Working principle of the RSS.

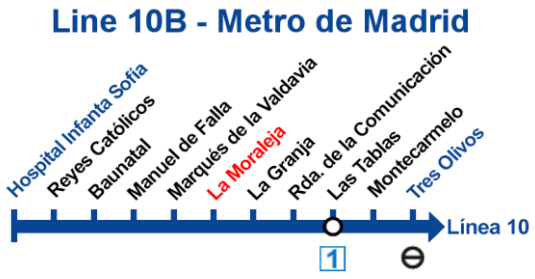

Fig. 2. The 11 stops of the line 10B.

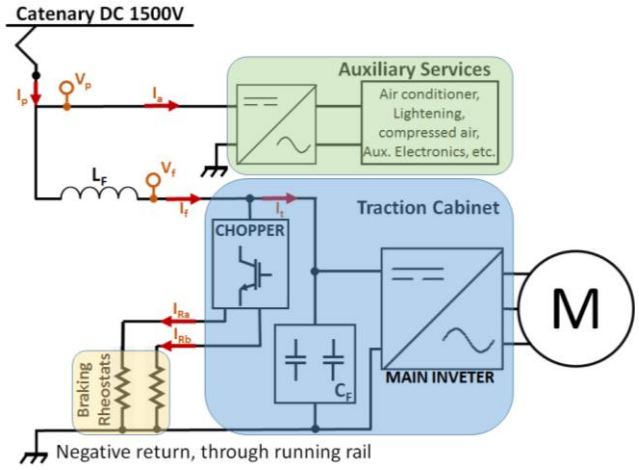

Fig. 3. Electric diagram of the traction carriage of S9000.

Fig. 3 provides a simplified diagram of the power input stage of the monitored unit. The energy absorbed by the pantograph is shared by two loads: the traction energy, that represents the main load, and the auxiliary services, which consists of the sum of all the other loads on board (air conditioner, illumination, electric door, and other electric and electronic on-board systems).

The inductance L_f and the capacitor bank C_f compose a second order filter necessary to limit the voltage distortion [28] coming from the line (V_p) to the inverter (V_f) during traction, and, at the same time, to limit the current distortion injected by the inverter in the supply line during the energy recovery due to the braking events. During a dynamic braking, the level of V_f (and thus also V_p) increases to inject energy into the supply line, as described before, if there is another train available to absorb it. When the generated energy cannot be completely injected in the line, two resistor banks, connected in parallel to the traction inverter, are supplied to dissipate on board the surplus of energy. A chopper, series connected to the resistors, modulates their energy dissipation on the base of the required braking effort and the availability of the line to receive energy.

The average values of the currents in the rheostats, I_{Ra} and I_{Rb}, can be regulated adopting a Pulse Width Modulated (PWM) strategy thus by changing the duty-cycle of absorbed current pulses. For the considered train, the frequency of PWM is about 300 Hz, the rated peak current amplitude is 600 A and the duty-cycle varies from 2 % to a maximum of 50%. At the minimum duty-cycle, the current pulses last about 66 µs. By varying the duty-cycle it is possible to manage the flow of braking energy by directing it towards the rheostats to be dissipated rather than towards the power supply line to be recovered. The control variable for this process is V_f: when it exceeds a specific threshold (for the considered train, a threshold of 1700 V was deducted by experimental evidence) the chopper begins to gradually increase the dissipation on-board so decreasing the current injected in the supply line and thus reducing the voltage level till a safe operating value.

III. MEASUREMENT SETUP

To perform a complete analysis of energy flows of the train during all operating conditions, the monitored quantities are (see Fig. 3): V_p – the voltage at pantograph, V_f – the filtered voltage that is the voltage applied on the two braking rheostats and also the traction inverter, I_p – the total current at pantograph, I_f – the traction cabinet input current, I_a – the auxiliary systems current, in the end, I_{Ra} and I_{Rb}, – the currents in the braking rheostats. The inside of the traction cabinet is not accessible, for this reason I_t, that is the current at the input of the main inverter, has been indirectly determined as it will be described in the following section.

The main energy exchange is at low frequency (basically DC) except for the energy dissipated by braking rheostats that adopt a PWM technique. For this reason and for being able to perform more insight analyses (i.e. fast transients occurring at the pantograph such as arc events [29]), the adopted measurement system has been designed to perform large bandwidth analyses (up to tens of kilohertz). The measurement system is able to acquire and to store two voltages and five currents (see Fig. 4). It is based on a National Instruments Compact Rio 9034 that is a stand-alone reconfigurable embedded chassis, that features an embedded controller with a 1.91 GHz real time processor, a reconfigurable (Field Programmable Gate Array) FPGA, 2 GB RAM DDR3 and a SD port for data storage. As regards the acquisition modules, the Compact Rio houses two NI 9223 that are 4-channel voltage modules, with differential inputs and simultaneous sampling with a maximum range of ± 10 V, 1 MHz as maximum sampling rate and a resolution of 16 bit. The data acquisition is performed at a sample rate of 50 kHz. The acquisition system is referenced to absolute time via the GPS module NI 9467, that provides a Pulse Per Second (PPS) signal with an accuracy of 100 ns. Obviously, the GPS receiver cannot work well underground, but the train passes in an open sky track at least once a day, the system can synchronize with UTC in that moment and then it keeps time using internal real time clock until next synchronization.

Two Ultravolt 40TF-CDCD (40 kV/40 V 0 Hz ÷ 1 MHz, 0.25 %) resistive-capacitive compensated dividers have been adopted to scale down the voltages V_p, and V_f which nominal amplitude is 1500 V. Open loop Hall effect current transformers have been used for the currents. They have openable magnetic core, that facilitate the installation. Two different models have been used, the HOP 2000 and the HOP 800 from LEM with 2000 A and 800 A of primary nominal current respectively.

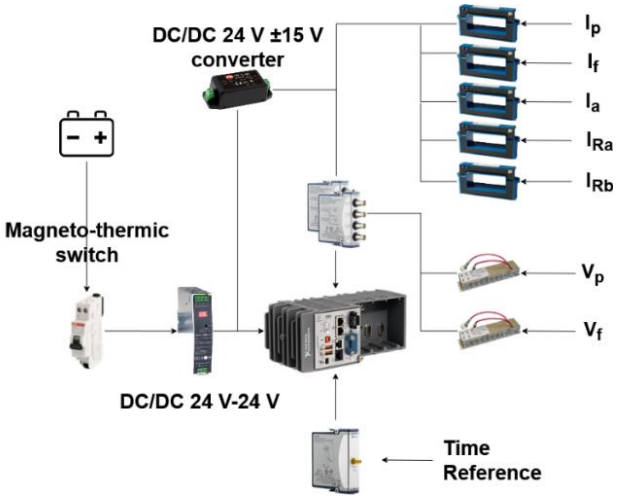

Fig. 4. Measurement setup.

The former has been used for I_p and I_f, whose amplitudes can reach 1000 A. The latter instead is used for I_a, I_{Ra} and I_{Rb} as they reach significantly lower amplitudes (600 A for I_{Ra} and I_{Rb}, less than one hundred of ampere for I_a). Both models feature an accuracy better than 2 % and a flat frequency response from DC to 10 kHz. The measurement system and the transducers are battery powered in order to allow a continuous monitoring of the train signals, even when the pantograph is not in contact with the catenary.

The data acquisition system has been located in the low voltage cabinet. The voltage divider related to the pantograph voltage measurement and the current transducer related to the auxiliary service current have been installed in the high voltage cabinet. The other transducers are located under the train in proximity of the traction cabinet. All the transducers adopted have been metrologically characterized at INRIM laboratories to guarantee traceability. The calibrations were carried out in stationary conditions at various levels of amplitude. DC gains and offsets were accurately assessed with an expanded uncertainty of 250 ppm for voltage and 150 ppm for current, both gain and offset, with a confidence level of approximately 95 % (k = 2). All measurements were compensated using the transducers gains obtained by the laboratory calibration results. Even though other influence factors affect the uncertainty associated with the on-site measurements, the on-field estimated accuracy is about 1%. For what concerns the measurement of the current flowing in the braking rheostats, an accurate measurement model, described in [31], has been applied.

The analysis of the DC energy flows has been carried out in agreement with the following relations. By the Kirchhoff's current law applied to the circuit shown in Fig. 3, we can write:

$$\begin{cases} I_p = I_a + I_f \\ I_f = I_R + I_t \end{cases} \quad (1)$$

where I_R is the total current dissipated in the rheostats:

$$I_R = I_{Ra} + I_{Rb} \quad (2)$$

while I_t is determined by:

$$I_t = I_f - I_R \quad (3)$$

The overall balance of the DC energies results:

$$E_p = E_a + E_L + E_t + E_D \quad (4)$$

where E_p is the total energy absorbed at pantograph, E_a is the energy absorbed by the auxiliary systems, E_L is the energy dissipated by the input filter, E_t is the energy absorbed by traction system and E_D is the energy dissipated by the braking rheostats. These energies are obtained by implementing the following equations:

$$E_p = \int_{t_1}^{t_2} V_p(t) \cdot I_p(t) \cdot dt\,; \quad (5)$$

$$E_a = \int_{t_1}^{t_2} V_p(t) \cdot I_a(t) \cdot dt \quad (6)$$

$$E_L = \int_{t_1}^{t_2} (V_p(t) - V_f(t)) \cdot I_f(t) \cdot dt\,; \quad (7)$$

$$E_t = \int_{t_1}^{t_2} V_f(t) \cdot (I_f(t) - I_R(t)) \cdot dt\,; \quad (8)$$

$$E_D = \int_{t_1}^{t_2} V_f(t) \cdot (I_{Ra}(t) + I_{Rb}(t)) \cdot dt\,; \quad (9)$$

where t_1 and t_2 are the start and the end of the considered time interval (5-9).

During acceleration, coasting and stop stages ($I_t \geq 0$) E_r (and I_R) is equal to zero as rheostats do not operate and all the other quantities in (4) are positive. The auxiliaries play a marginal role typically with an almost constant absorption and that is in any case much lower than peak value of E_t. Also E_L is a small percentage of E_t.

During the braking, the energy flow is inverted: E_t becomes negative (energy is generated by the motors). In this condition, it can be useful to define the braking energy as $E_{br} = -E_t$ and the injected energy as $E_{in} = -E_p$ thus (4) can be rewritten with all positive terms as

$$E_{br} = E_a + E_L + E_D + E_{in} \quad (10)$$

A part of the E_{br} is typically recovered by the auxiliary systems on-board train; this is the easiest way to recover energy net of filter losses (E_L). Any additional energy can be injected (E_{in}) in the supply system, net of E_L, if there are some other devices nearby able to use this energy at that very moment. Otherwise, the consequence of the energy injection is the increase of pantograph voltage, till exceeding its normal range. When this condition occurs, to avoid damages provoked by overvoltage, the control system starts increasing the on-board dissipation in the braking rheostats (E_D) to reduce the amount of E_{in}, so taking back the voltage level under a specified safety threshold. As a consequence, it is possible that E_{br} is all injected, partially injected and partially dissipated or even all dissipated on-board, depending on the availability of the line to receive energy (line receptivity). The expected impact of a reversible substation is the improvement of the line receptivity. To analyse these aspects with experimental data, the authors propose a new parameter, L_u (Line unavailability seen by point of view of train), defined as:

$$L_u = 100 \cdot (E_D / E_{br}) \quad (11)$$

This parameter is inversely proportional to the receptivity of the line and so, in the following, it will be used as index of unavailability of the line to accept energy.

As the line unavailability changes with time, it can be useful to express the relation that links the L_u with the average power of the braking. In fact, introducing t_{br}, the duration of the considered braking event, the average power that is dissipated ($\bar{P}_D$) and generated ($\bar{P}_{br}$) during the braking can be calculated as:

$$\bar{P}_D = \frac{E_D}{t_{br}} \quad (12)$$

$$\bar{P}_{br} = \frac{E_{br}}{t_{br}} \quad (13)$$

and thus (11) can be rewritten as

$$L_u = 100 \cdot (\bar{P}_D / \bar{P}_{br}) \quad (14)$$

Consequently, this parameter is independent by the duration of braking. Moreover, as the braking power and energy are expected to be independent on the presence of RSS, the statical variability of this parameter is expected to be only dependent on the number of trains, the required braking effort,

and the presence of RSS. By analysing a large number of braking events over a long-time interval, the statistics obtained can be considered representative of all working conditions. This type of analysis can be carried out separately in both power supply configurations (RSS ON and OFF), and, since the other influencing factors have statistically the same impact, by comparing the variation of the statistical parameters of L_u it is possible to highlight the effect of RSS.

IV. EXPERIMENTAL RESULTS

Since October 2019, a measurement campaign has been performed for 18 days by monitoring, in a continuative way, a train operating only on the line 10B covering in a repetitive and comprehensive way all the working conditions of the line in terms of traffic density and time slots. Information about 350 roundtrip journeys have been acquired and over 500 GB of data have been stored. Almost in half of the monitored time the RSS was active, while in the other half it was not operating (121 and 111 working hours respectively). In both the situations all the working conditions are covered in a similar way, so statistical analyses can be performed obtaining comparable results.

In Fig. 5 the traction current obtained by (2) is reported as example of a typical journey form Hospital Infanta Sofia to Tres Olivos. The time intervals corresponding to the ten movements of the train between consecutive stations (sub-tracks) are highlighted: it is possible to recognize the acceleration stages leaving from the stations (big positive current spikes) and the braking stages approaching to the next stations (big negative current spikes). After the braking, the train stops (I_t goes almost to zero) for a while in each station before leaving again.

The movement of the train was not always regular and sometimes the train driver had to brake before approaching the station, probably either approaching a bend or, alternatively, due to the presence of another train that had not yet left the next station (see Fig. 5 sub-track 4 – 8, starting from the first green dashed line). In the last part there is a speed limitation that consequently limits the current absorption.

The train tries to inject energy in the supply system during all the braking events but as previously described, the energy actually fed in the catenary firstly depends on the presence of a contemporary absorption (traction) of some other trains that are nearby. If this favourable condition does not occur, the regenerated energy should be transferred to the RSS. When the supply line has not the capability to absorb all the generated energy, the excess part must be dissipated on-board the train by the rheostats.

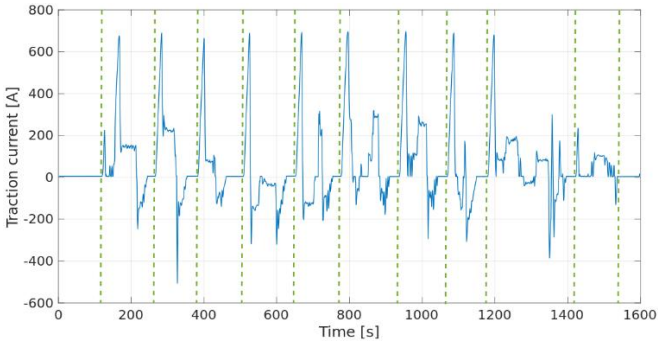

Fig. 5. Traction current (I_t) during a one-way trip.

This depends on the state of the other trains (e. g. other regenerative braking at the same time) or from the general dynamic state of the supply line (e.g. distance from regenerative substation or distance from other trains). The lack of receptivity of the supply line was detected by an excessive increment of the feeder voltage that triggers the on-board dissipation.

About 6951 braking events were identified and analysed, and to show the time evolution of the main electrical signals involved, Fig. 6 and Fig. 7 report two examples of braking events. These two events, even if with similar duration, are very different form an energetic point of view: the first one is the most regenerative, while the second one is the most dissipative among that provided by the measurement campaign.

The reported values are averaged over $\Delta t = 10\,ms$ that is enough for dynamic of almost all signals, except for I_R that, as previously stated, is a chopped current at 300 Hz. Therefore, for this signal, both the current sampled at 50 kHz and its average value over 10 ms are reported (red and black line respectively). Both figures confirm the expected control system behaviour: when V_f overcomes the threshold of 1700 V (dotted yellow line), the chopper starts the dissipation in the braking rheostats ($I_{R\ samples} \neq 0$, red line). It can be noticed that, even if the peak levels of current are nearly constant ($I_{R\ samples}$ red line), the average value of I_R (black line) is not constant, because it depends on the duty-cycle of the chopper. This is not appreciable with instantaneous values graph. The black line shows how the amount of energy changes in agreement with braking effort and line receptivity.

Fig. 6 provides an intense braking (E_{br}= 5.11 kWh) in which the energy has been almost all injected (E_{in}= 4.60 kWh). In fact, I_f always assumes negative and large values while I_R always maintains low values (less than 20 A). So that only a small amount of energy is dissipated on board while most of the energy is injected into the line. The details about this event, including the amounts of involved energies, are reported in the first row of Table 2 where the information about the four braking events with the highest amount of E_{in} are reported.

Fig. 7 reports a braking with medium effort (E_{br}= 3.17 kWh) in which the energy has been almost all dissipated on-board (E_d= 2.53 kWh). Please note that just after the start of braking (at second 0.4) V_f exceeds the threshold and it keeps over that level till the end of the event.

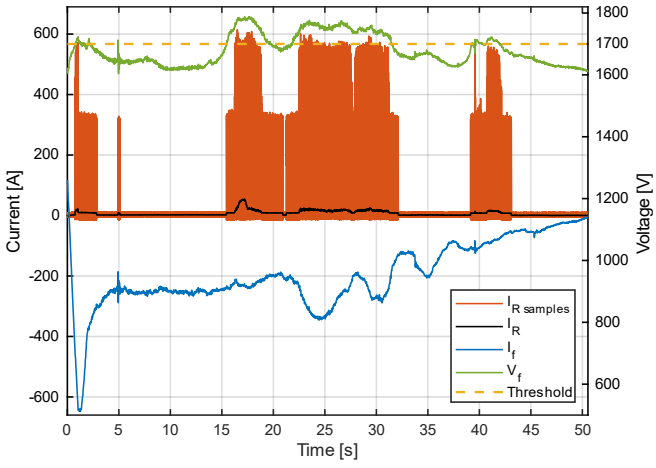

Fig. 6. Main signals during the most regenerative braking.

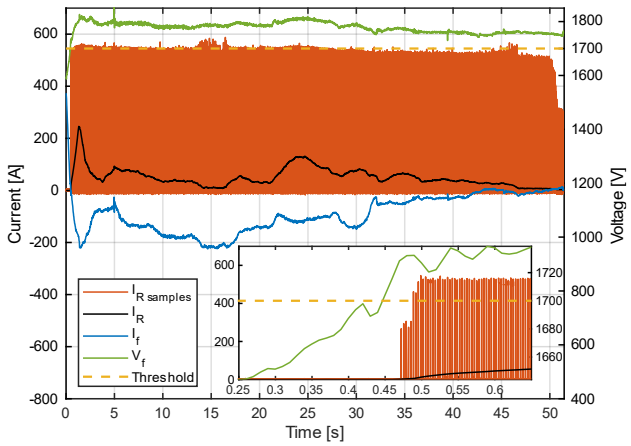

Fig. 7. Main signals during the most dissipative braking.

I_R assumes large values peak value of 250 A) while I_f always maintains low values (peak value of -220 A). This is the consequence of a low line receptivity, maybe due to the simultaneous braking of another train. The details about this event including the amounts of involved energies are reported in the first row of Table 1 where the information about the four brakings with the highest amount of E_d are provided. Some considerations can be done comparing Table 1and Table 2. Firstly, it can be noticed that for all the cases of high reinjected energy, the RSS is active. On the other hand, all the most dissipative braking events happen when the reversible part is switched off, coherently with what can be expected. Moreover, looking at the 5th column of Table 2, the most regenerative braking events occur when there is a bigger number of trains with respect to those in Table 1. As expected, the line receptivity is not constant and can be related to the number of trains simultaneously present on the line, but the presence of the reversible part impacts as well. In fact, one of the most regenerative events occurs with only 6 trains (second row of Table 2); obviously, it could not only be due to the RSS, because there is a not negligible probability to have at least one of the other five trains accelerating simultaneously. A complete evaluation of the RSS impact cannot be performed by analysing single events. Only the statistical approach, described in the following, provides significant results.

A. Impact of RSS in terms of energy efficiency

As already stated before, the train was monitored with the RSS that, in the first half of time, is active, and in the other half is not operating. In the following, for sake of brevity the first condition will be referred as "Reversible substation" and the second as "Conventional substation". In both the situations all the working conditions of the train are covered in a similar way, so statistical analyses carried out in the two periods provide comparable results.

One of the advantages expected by the adoption of a RSSs is a more stable supply voltage [30].

Table 1. The most dissipative braking events of the campaign

Date	Time	t_{br} [s]	RSS state	Circulating Trains	E_{br} [kWh]	E_D [kWh]
21-oct	01:56	50	OFF	3	3.17	2.53
21-oct	01:09	50	OFF	3	4.84	2.24
19-oct	07:54	37	OFF	7	5.00	2.17
19-oct	12:07	40	OFF	7	4.85	1.99

Table 2. The most regenerative braking events of the campaign.

Date	Time	t_{br} [s]	RSS state	Circulating Trains	E_{br} [kWh]	E_{in} [kWh]
15-oct	06:23	50	ON	6	4.82	4.60
15-oct	06:36	85	ON	8	5.11	4.59
7-oct	18:57	50	ON	11	4.74	4.55
11-oct	11:13	50	ON	9	4.87	4.55

To analyse this aspect, Fig. 8 provides a comparison of the different statistical distributions of V_{f}, obtained with conventional and reversible substation. This parameter was chosen, in place of V_{p}, because, as mentioned before, it is the control variable that manages the amount of dissipated energy in the on-board rheostats. More in details, two Probability Density Functions (pdf) are obtained considering the average voltage level during each braking event.

The two distributions shown in Fig. 8 have a bimodal behaviour with intersection in correspondence of the chopper intervention threshold (see black dashed line). There are very similar, and the expected improvement is not so evident. This could be due to several reasons: the limited amount of the power injectable in AC side, the presence of only one RSS over 5 substations, that entails a higher average distance between train and RSS, and the high level of the supply voltage that is really near to the threshold level of the braking chopper. Nevertheless, some improvement in voltage stability can be noted: there is a reduction of the mean value (from 1690 V to 1682 V) and of the 95th percentile value (from 1771 V to 1767 V). In practice, the presence of the RSS limits the occurrences of voltage level over 1700 V. Anyway, the similarity of the two distributions confirms the comparable working conditions of the two considered situations.

An important role in the energy recovery is played by the effective amount of the braking power. As previously said, this parameter is expected to be practically constant in the considered two supply conditions since it is not dependent on the presence of RSS. Furthermore, the presence of Automatic Train Operation (ATO) leads to expect a repetitive behaviour during braking. In fact, Fig. 9 provides a comparison of the different statistical distributions of P_{d} measured during the braking events, with conventional and reversible substation: the two pdfs almost completely overlap. The pdf shows three picks at 56 kW, 160 kW and 230 kW that represent the most common braking power efforts. The impact of the RSS is evaluated by some statistical analysis of L_{u}, the line unavailability to receive energy (see (11) and (14)).

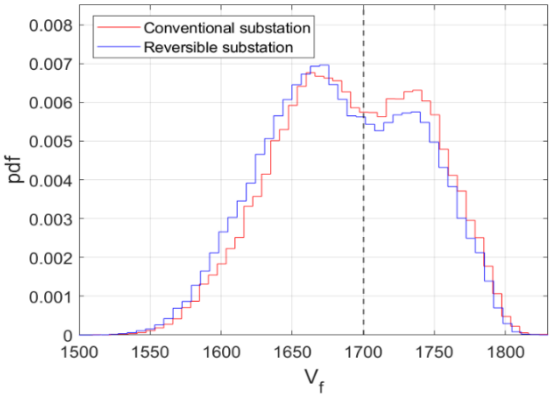

Fig. 8. Comparison of statistical analysis of the voltage during braking events.

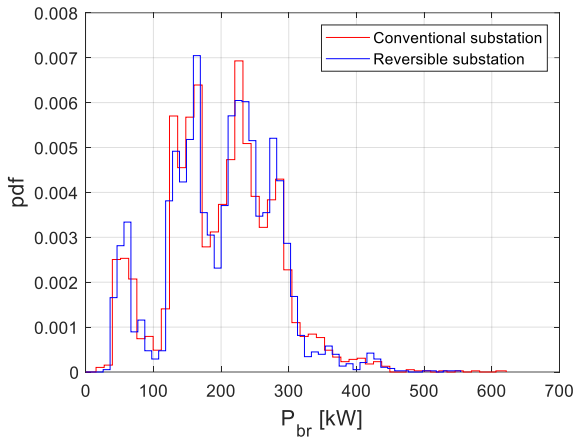

Fig. 9 Comparison of statistical analyses of braking power

The measured values of L_u are analyzed by the pdf and the Cumulative Distribution Function (cdf) and by some synthetic indexes such as average, standard deviation and 95th percentile.

The first analyses have been conducted over all the working hours, considering separately all the braking events recorded when the RSS is ON (Fig. 10a) and OFF (Fig. 10b).The two distributions have a very similar behaviour but the presence of RSS produces a significant reduction of the synthetic statistical parameters associated with L_u. In particular, the average is reduced by about 20 % and 95th percentile and standard deviation are reduced by about 10%.

To show how the different traffic conditions affect L_u, the same statistical analyses of Fig. 10 were performed over the braking events that occur in specific hours. In fact, using the timetable of Metro de Madrid it has been possible to know, at the different hours of each day, the number of trains that are contemporary in service. Therefore, comparative analyses were again performed but considering separately the braking events that happen in the time slots with high traffic (number of circulating trains ≥ 9) and with low traffic (number of circulating trains ≤ 3). The results are reported in Fig. 11 and Fig. 12, respectively.

The shapes of distributions in Fig.11 are very similar to those in Fig.10 and the most probable values are those with low L_u amplitude (in both cases the 95th percentiles are about 30% and the most probable values are close to 5%). More different are the distributions shown in Fig. 12: Higher amplitudes of L_u are more probable (the 95th percentiles are over 40% with a more uniform distribution). This is an expected behaviour because the number of trains directly impacts on L_u: the greater the number of trains, the greater the receptivity of the line.

The presence of RSS in both situations (compare Fig. 11a with 11b and Fig. 12a with 12b) increases the probability to have lower values of L_u and, in fact, all synthetic indexes sensibly reduce their value.With high receptivity (Fig. 11 a and b) the difference between conventional and reversible is about 2 % for the mean value and 3.6 % for the 95th percentile, that is almost aligned with the results in Fig. 10.

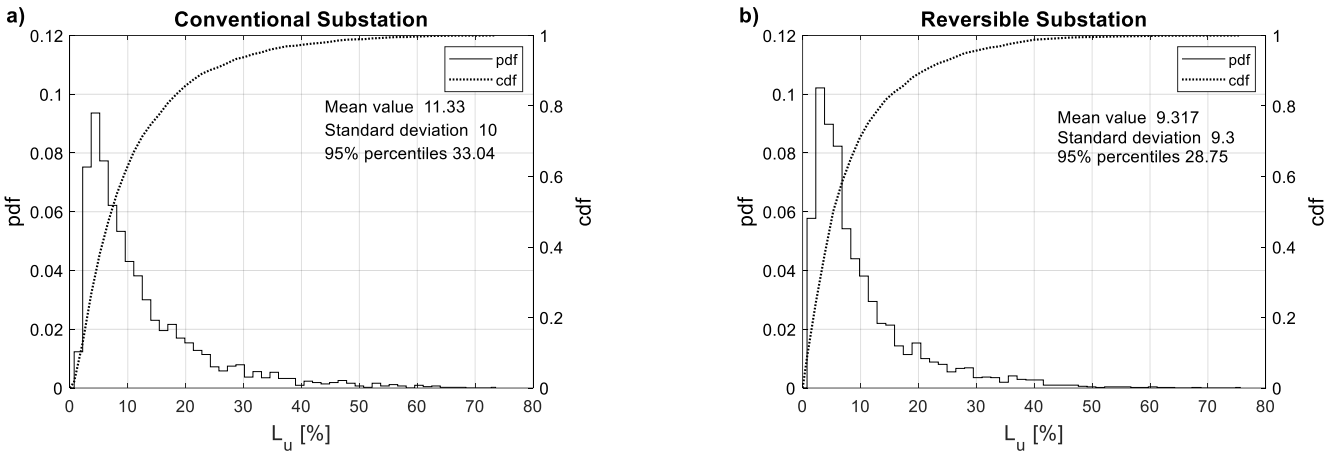

Fig. 10. Line unavailability statistic by considering conventional substation a) and RSS b).

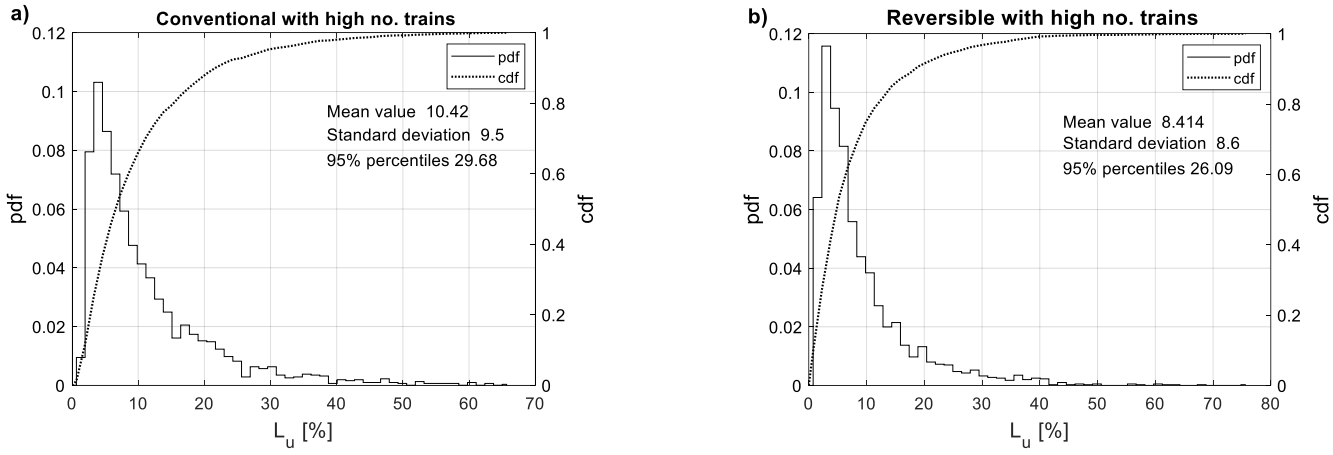

Fig. 11 Line unavailability statistic with high number of trains (≥9) by considering conventional substation a) and RSS b).

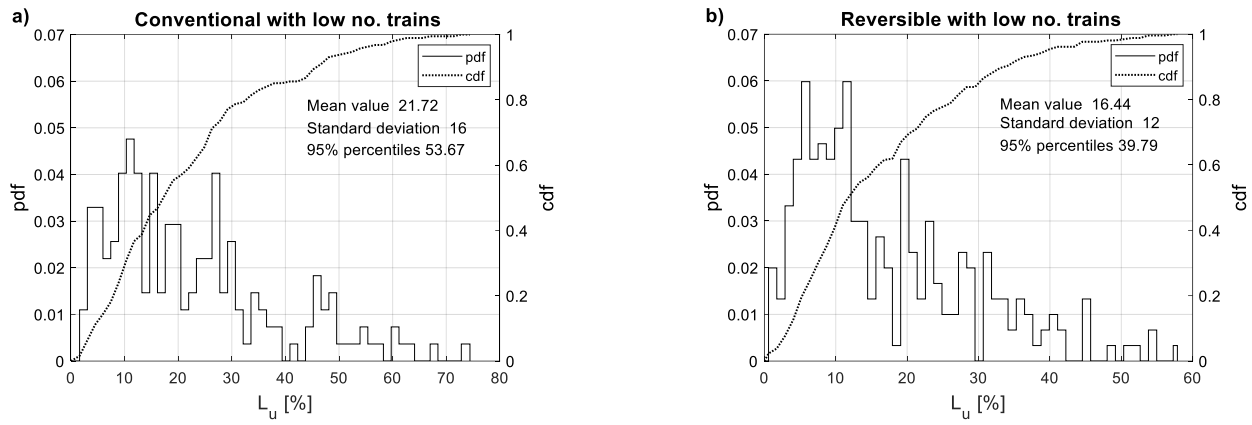

Fig. 12. Line unavailability statistic with low number (≤3) of trains by considering conventional substation a) and RSS b).

With low receptivity (Fig. 12a and b) the difference between conventional and reversible is more remarked, it reaches about 5.3 % for the mean value and 13.9% for the 95th percentile. It is interesting to note that with lower circulating trains (see Fig. 12), the effect of the RSS is more evident: the synthetic indexes reduction is much greater than in Fig. 11 and the shape of distribution in Fig. 12b becomes more similar to those in Fig. 10 and 11. This occurs because with a low number of trains during braking there is less chance that another train is accelerating at the same time and absorb the regenerated energy; therefore, energy recovery is much more reliant on RSS.

To quantify with absolute values the impact of the RSS in the same situations considered in Fig. 10, 11 and 12, in Table 3 the corresponding average values of E_D are reported (first second and third column, respectively).

As it can be noticed from the first column, the presence of the RSS allows a reduction of 21.4 % of the on-board dissipation (passing from 202 kWh to 159 kWh).

Table 3. Analysis of the Dissipated Energy

Traffic Conditions	**All**	**Train n. ≥ 9**	**Train n. ≤ 3**
Average E_D [kWh] Conventional	202	183	427
Average E_D [kWh] Reversible	159	145	296
Relative Increment [%]	21.4	20.9	30.7

Nearly the same behavior was found with high number of trains (compare the first and the second column), because the line receptivity is kept high by the presence of many trains and the RSS has only a minor impact. On the contrary, the effect of RSS is very evident observing the values of the third column. In this case the relative increment reaches the 30.7 %. As noted in the Section III, the voltage level is an important parameter involved in on board dissipation and thus with L_u level. The voltage level during all the identified braking events is considerably high compared with the nominal value of 1500 V, as it can be seen by the statistics of Fig. 8. This is a consolidated practice in railways systems. A higher voltage level allows to reduce Joule effect losses in train supply, but it is supposed also to limit the amount of energy that could be injected and thus increasing the line unavailability. In order to evaluate the influence that the voltage level could have on L_u, Fig. 13 and Fig. 14 shows a scatter chart of L_u with respect to the ratio between voltage level during the braking (V_p) and nominal line voltage (V_n). In particular, the voltage has been determined for each braking event in correspondence of the peak injected current to emphasize the relation between voltage and L_u.

This analysis was conducted in a similar way to what was done previously, so the results obtained with a high number of trains are reported with reference to conventional and reversible substation in Fig. 13 a and b, respectively. Similarly, Fig. 14 shows results obtained with low number of trains.

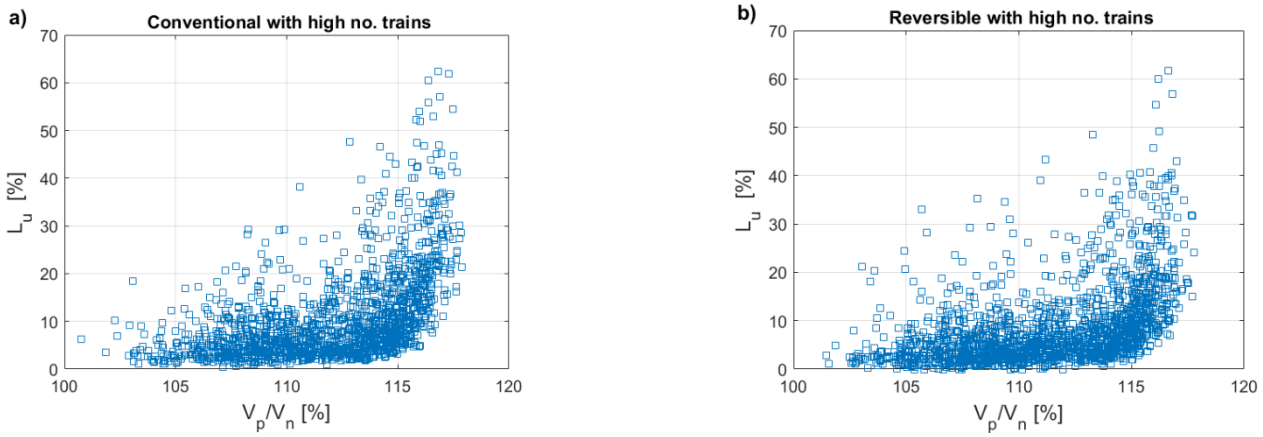

Fig. 13. Scatter chart of line unavailability versus measured voltage level with high number of trains (≥9) by considering conventional substation a) and RSS b).

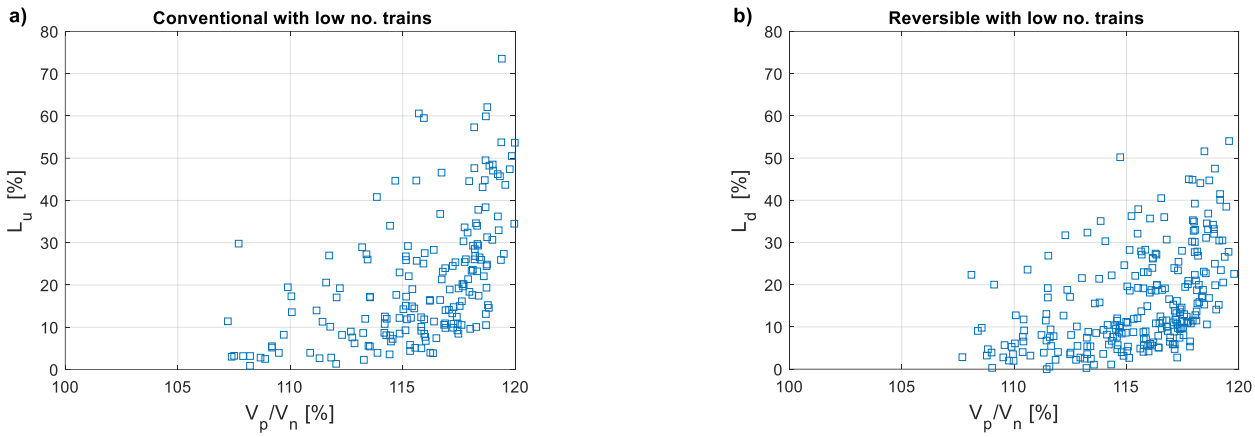

Fig. 14. Scatter chart of line unavailability versus measured voltage level with low number (≤3) of trains by considering conventional substation a) and RSS b).

Comparing the four charts, it can be seen that the dots move to the right and to the top for lower receptivity and conventional conditions. To simplify the comparison between the reversible and conventional case, an exponential interpolation of such a scatter has been performed. Even if the interpolation is not a good representation, because the data are quite scattered, the exponential could represent, theoretically, the relationship between L_u and the voltage level.

The results are reported in Fig. 15 a and b respectively for low and high receptivity. As it can be seen, they confirm the impact of the RSS in both cases. As expected, the difference between reversible condition and conventional one is greater in low receptivity than high.

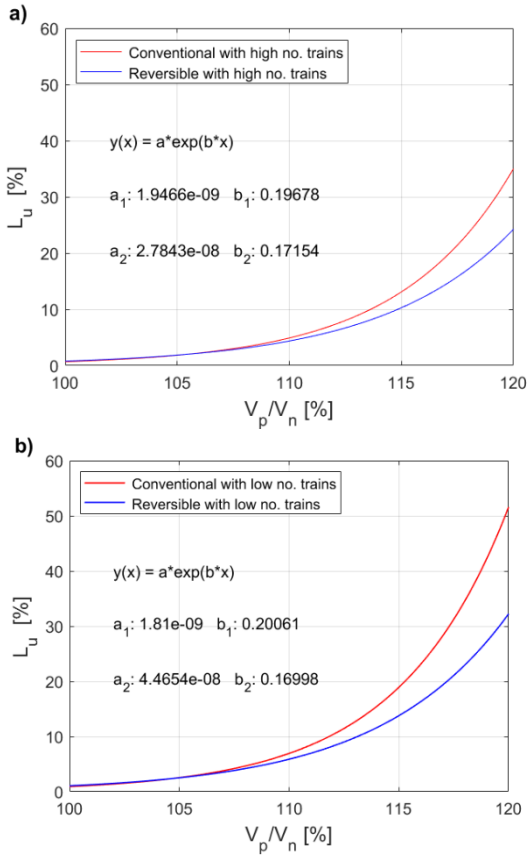

Fig. 15. Exponential fittings in correspondence of a high a) and low b) number of trains.

Moreover, for both conditions, at high voltage levels there is a greater impact of the RSS. The curves reported in Fig. 15 can be also used to analyse which would be the impact of a reduction of a supply voltage in terms of reduction of L_u. It is evident that with the presence of a RSS, higher levels of the supply voltage can be adopted without a sensible increment of L_u.

B. Energy flow analysis

In Table 4 the results of a comprehensive energy analysis of a week, in which the reversible unit is operating, is reported. As stated before, the measurements are conducted on single traction unit, so they should be doubled to have the values for all the train. At the pantograph, the absorbed ($I_p > 0$) and the injected ($I_p < 0$) energies are evaluated separately and reported together with the net amount of energy. The average value of the recovery factor was about 38%. During braking stage, as expected, most of the energy is recovered; nevertheless, an average amount of 9% of regenerated energy is dissipated on board. The auxiliary services have a minor impact on energy balance, and they just cover the 5% of the absorbed power. The loss in the input filter (2%) has low influence too.

It is possible to calculate the average flows of power, starting from the totals of energies in Table 4 and averaging over working hours (see Fig. 16). During absorption periods ($E_p > 0$), the single traction unit works as a load with an average power absorption of about 105 kW (blue arrows) and almost all the power goes for traction: $E_R = 0$, the auxiliary absorption and filter dissipation gives limited contribute.

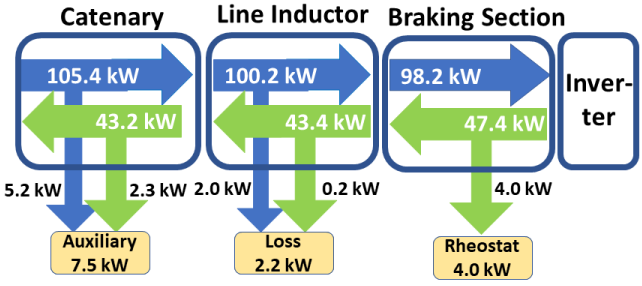

Fig. 16. Average energy flow over working hour for single traction unit.

Table 4 Energy monitoring results in reversible conditions.

Date	Working hours	number of routes	Input energy (kWh)			Braking energy (kWh)			*Auxiliary Services* (kWh)			Input filter (kWh)		
			Absorbed	*Injected*	*Net Absorbed*	*Generated*	*Dissipated*	*Net Recovered*	*Total*	*Braking Phase*	*Traction Phase*	*Total*	*Braking Phase*	*Traction Phase*
4 - oct	20:46	27	2266	-857	1408	985	65	920	206	54	151	46	5	41
5 – oct	20:44	26	2124	-816	1308	946	84	862	117	35	82	49	4	44
6 – oct	16:36	21	1626	-613	1013	703	52	650	134	33	101	34	3	30
7 – oct	12:45	16	1366	-549	817	624	45	578	79	25	54	30	3	27
10 – oct	04:38	6	471	-194	277	215	11	204	24	9	15	9	1	8
11 – oct	20:18	26	2264	-919	1344	1065	96	969	119	43	76	51	6	45
12 – oct	9:25	12	1037	-385	652	475	62	413	92	27	65	22	2	20
15 - oct	16:26	21	1680	-635	1044	754	77	677	141	54	88	34	4	31

During the braking, the energy flow is inverted (green arrows): E_t becomes negative (the energy is generated by the motor) and, as a consequence of the line receptivity, the energy is partially dissipated in the braking rheostats (9%) and partially reused (91%). It is interesting to note that the recovered energy is partially absorbed by auxiliary systems, partially dissipated in the filter and the rest of the energy is fed back to the catenary.

V. CONCLUSION

This paper presented and discussed the results of a measurement campaign that has been conducted on-board of a train operating on the metro line that serves the city of Madrid, where a RSS was installed. At the best authors knowledge, it is the first article to provide real experimental data of this type.

A new index (L_u) that quantifies the line unavailability to receive energy was proposed. The impact of RSS was analysed by performing statistical analysis of a large number of braking events over a long-time interval taking into account separately different supply conditions (RSS on and off) and high and low circulating train number. Statistics show that in case of high traffic, L_u has an average value of 10% and 8% without and with the RSS respectively. Such percentages become 22 % and 16 % for the low traffic condition, giving evidence of the higher impact of the reversible substation when few trains are in service. The behaviour of L_u versus the actual and rated supply voltage, obtained by fitting the samples provided by each braking, clarifies that the impact of the RSS increases as such voltage ratio increases. Although the RSS is in experimental stage and the amount of energy sent back to the main grid is limited by the law in force, the results of this comparison show that the RSS adoption has potential to considerably improve the overall efficiency, in particular when the number of trains is low.

ACKNOWLEDGEMENTS

This research was funded by EMPIR program co-financed by the participating countries and the European Union's Horizons 2020 research and innovation program, project name MyRailS, grant number 16ENG04.

The authors wish to thank Hitachi staff for their valuable contribution in the instrumentation installation phase and during the experimental activity.

REFERENCES

[1] COM (2011) 144 Wight Paper: Roadmap to a Single European Transport Area – Towards a competitive and resource efficient transport system.

[2] Directive 2014/94/EU of the European Parliament and of the Council of 22 October 2014 on the deployment of alternative fuels infrastructure.

[3] https://ec.europa.eu/eurostat/databrowser/view/nrg_bal_c/default

[4] M. González-Gil, A.; Palacin, R.; Batty, P. Sustainable urban rail systems: Strategies and technologies for optimal management of regenerative braking energy. Energy Convers. Manag. 2013, 75, 374–388, doi:10.1016/j.enconman.2013.06.039

[5] M. Khodaparastan, A. A. Mohamed and W. Brandauer, "Recuperation of Regenerative Braking Energy in Electric Rail Transit Systems," in IEEE Transactions on Intelligent Transportation Systems, vol. 20, no. 8, pp. 2831-2847, Aug. 2019, doi: 10.1109/TITS.2018.2886809.

[6] Gelman, V. Braking energy recuperation. IEEE Veh. Technol. Mag. 2009, 4, 82–89, doi:10.1109/MVT.2009.933480.

[7] Fazel, S.S.; Firouzian, S.; Shandiz, B.K. Energy-Efficient Emplacement of Reversible DC Traction Power Substations in Urban Rail Transport through Regenerative Energy Recovery. 12. International Journal of Railway, 2014, volume 1 pp. 11–22.

[8] Y. Oura, Y. Mochinaga, H. Nagasawa, "Railway Electric Power Feeding Systems", Japan Railway & Transport Review 16, June 1998.

[9] A. Delle Femine, D. Gallo, C. Landi, M. Luiso, Discussion on DC and AC power quality assessment in railway traction supply systems (2019) I2MTC 2019 - 2019 IEEE International Instrumentation and Measurement Technology Conference, Proceedings, 2019-May, art. no. 8826869

[10] IEC 62313:2009 Railway applications - Power supply and rolling stock - Technical criteria for the coordination between power supply (substation) and rolling stock.

[11] M. Brenna, F. Foiadelli, D. Zaninelli, "Electrical Railway Transportation Systems", Mar 2018, Wiley-IEEE Press.

[12] H. Douglas, C. Roberts, S. Hillmansen, F. Schmid, "An

assessment of available measures to reduce traction energy use in railway networks," Energy Conversion and Management, Vol. 106, Dec. 2015, Pages 1149-1165

[13] Su, S., Wang, X., Cao, Y. and Yin J. An Energy-Efficient Train Operation Approach by Integrating the Metro Timetabling and Eco-Driving, IEEE Transactions on Intelligent Transportation Systems 2020, 21, 4252-4268

[14] Dominguez, M., Fernández-Cardador, A, Cucala, A. P. and Pecharroman, R. R., Energy Savings in Metropolitan Railway Substations Through Regenerative Energy Recovery and Optimal Design of ATO Speed Profiles, in IEEE Transactions on Automation Science and Engineering 2012, 9, 3, 496-504

[15] Popescu, M.; Bitoleanu, A. A Review of the Energy Efficiency Improvement in DC Railway Systems. Energies 2019, 12, 1092

[16] Z. Hou, H. Dong, S. Gao, G. Nicholson, L. Chen and C. Roberts, "Energy-Saving Metro Train Timetable Rescheduling Model Considering ATO Profiles and Dynamic Passenger Flow," in IEEE Transactions on Intelligent Transportation Systems, vol. 20, no. 7, pp. 2774-2785, July 2019, doi: 10.1109/TITS.2019.2906483.

[17] M. Peña-Alcaraz, A. Fernández, A. P. Cucala, A. Ramos and R. R. Pecharromán, "Optimal underground timetable design based on power flow for maximizing the use of regenerative-braking energy", Proc. Inst. Mech. Eng, vol. 226, no. 4, pp. 397-408, 2011.

[18] X. Yang, X. Li, Z. Gao, H. Wang and T. Tang, "A cooperative scheduling model for timetable optimization in subway systems", IEEE Trans. Intell. Transp. Syst., vol. 14, no. 1, pp. 438-447, Mar. 2013.

[19] A. Ramos, M. T. Peña, A. Fernández and P. Cucala, "Mathematical programming approach to underground timetabling problem for maximizing time synchronization", Proc. XI Congr. Ing. Org., pp. 1-8, 2007.

[20] A. Nasri, M. F. Moghadam and H. Mokhtari, "Timetable optimization for maximum usage of regenerative energy of braking in electrical railway systems," SPEEDAM 2010, 2010, pp. 1218-1221, doi: 10.1109/SPEEDAM.2010.5542099.

[21] W. Gunselmann, "Technologies for increased energy efficiency in railway systems," 2005 European Conference on Power Electronics and Applications, 2005, pp. 10 pp.-P.10, doi: 10.1109/EPE.2005.219712.

[22] M. Khodaparastan, A. A. Mohamed and W. Brandauer, "Recuperation of Regenerative Braking Energy in Electric Rail Transit Systems," in IEEE Transactions on Intelligent Transportation Systems, vol. 20, no. 8, pp. 2831-2847, Aug. 2019, doi: 10.1109/TITS.2018.2886809.

[23] D. Cornic, "Efficient recovery of braking energy through a reversible dc substation," Electrical Systems for Aircraft, Railway and Ship Propulsion, Bologna, 2010, pp. 1-9, doi: 10.1109/ESARS.2010.5665264

[24] G. Crotti et al., "Monitoring Energy and Power Quality On Board Train", 2019 IEEE 10th International Workshop on Applied Measurements for Power Systems (AMPS), 2019, pp. 1-6, doi: 10.1109/AMPS.2019.8897794.

[25] Ortega JM, Ibaiondo H. Kinetic energy recovery on railway systems with feedback to the grid. In: 9th World congress on railway research (WCRR), Lille; 2011.

[26] F. Cascetta, G. Cipolletta, A. Delle Femine, D. Gallo, D. Giordano, D. Signorino, "Measuring the impact of reversible substations on energy efficiency in rail transport", *IMEKO TC4 Conference,* September 2020

[27] EURAMET Joint Research Program "Metrology for Smart Energy Management in Electric Railway Systems" 16ENG04 MyRailsProject

[28] A. Delle Femine, D. Gallo, D. Giordano, C. Landi, M. Luiso, D. Signorino, "Power Quality Assessment in Railway Traction Supply Systems", 2020 IEEE Transactions on Instrumentation and Measurement, 69(5), 8962225, pp. 2355-2366

[29] G. Crotti, A. Delle Femine, D. Gallo, D. Giordano, C. Landi, M. Luiso, A. Mariscotti, P. Roccato "Pantograph-to-OHL Arc: Conducted Effects in DC Railway Supply System", IEEE Transactions on Instrumentation and Measurement, 2019.

[30] Kleftakis, V. A, Hatziargyriou, N.D. Optimal control of reversible substations and wayside storage devices for voltage stabilization and energy savings in metro railway networks. IEEE Transactions on Transportation Electrification 2019, 5(2), 515-523.

[31] Giordano, D.; Signorino, D.; Gallo, D.; van den Brom, H.E.; Sira, M. Methodology for the Accurate Measurement of the Power Dissipated by Braking Rheostats. *Sensors* 2020, *20*,6935.